Supplementary Material (ESI) for Chemical Communications

Supporting Information

Templated display of biomolecules and inorganic nanoparticles by metal ion-induced peptide nanofibers†

Byoung-Chul Lee and Ronald N. Zuckermann*

Biological Nanostructures Facility, The Molecular Foundry, Lawrence Berkeley National Laboratory, 1 Cyclotron Rd., Berkeley, CA 94720, USA

E-mail: rnzuckermann@lbl.gov; Fax: +1 510-495-2376; Tel: +1 510-486-7091

Materials and Methods

Synthesis of peptides with N-terminal N-(-*S*-1-carboxyethyl) substituted glycine. The peptides modified by N-terminal N-(*S*-1-carboxyethyl) glycine were synthesized on the Aapptec Apex 396 synthesizer (Louisville, KY). We used a solid-phase standard Fmoc chemistry for peptide synthesis and subsequent submonomer cycle[1] for N-terminal modification by N-(*S*-1-carboxyethyl) glycine. The Rink amide resin (0.57 mmol/g, Novabiochem, San Diego, CA) was used to generate a C-terminal amide. The Fmoc group from the Rink resin was first deprotected with 20 % 4-methlypiperidine in dimethylformamide (DMF). For the peptide synthesis, 2 mL of 0.4 M of Fmoc-protected amino acids in N-methylpyrrolidinone (NMP) was added to the resin-bound amine with 0.4 M hydroxybenzotriazole (HOBT) and 137 μL of DIC (0.92 mmol). The reaction mixture was incubated at room temperature for 2 hours. The Fmoc group from N-terminal amino acid was then deprotected with 20 % 4-methlypiperidine in DMF. Between the amide coupling and the deprotection, the resins were washed with 5 times of DMF. To modify the N-terminus of peptides with N-(*S*-1-carboxyethyl) glycine, the submonomer cycle was employed by bromoacetylation and amine displacement as described previously.[1] We added 1 ml of 1.5 M of the free base, (L)-*O*-t-butyl-alanine (Bachem) for N-(*S*-1-carboxyethyl) glycine at the N-terminus of compounds **1**, **2** and **3** during the amine displacement. All solvents and reagents were obtained from commercial sources and used without further purification.

The crude products (50 μmol of resin) were cleaved from the resins with 95:2.5:2.5 trifluoroacetic acid (TFA)/triisopropylsilane(TIS)/water (v/v) for 2 hours at room temperature. The cleavage solution was filtered and evaporated under a stream of nitrogen to remove the TFA. The crude product was then dissolved in a mixture of 9:1 water/acetonitrile. The aggregation from TIS and protecting groups was removed by filtration and subjected to further purification by reverse-phase HPLC with a Varian Dynamax C18 column (10 μm, 21.4 mm x 250 mm). All final products were analyzed by analytical reverse-phase HPLC (0–50 % gradient at 1 mL/min over 30 min at 60 ^{o}C with a Grace Vydac C18 column for purity and MALDI mass spectrometry (Applied Biosystems TF4800 MALDI-TOF-TOF Mass Spectrometer) for identity. Final products were lyophilized, dissolved in aqueous 10 mM NaOH and stored at -70 ^{o}C. Approximate

concentrations of products were determined by weight after lyophilization. All peptides were purified to more than 95 % purity by the analytical HPLC. The molecular weights determined by the MALDI mass spectrometry are listed in Table S1. The analytic HPLC profile and the MALDI mass spectrum for the compound **3** are shown in Figure S1.

Table S1. Molecular weights for the peptides modified with N-terminal N-carboxyethyl substituted glycine determined by the MALDI mass spectrometry.

peptide-peptoid hybrid	molecular weight (cal.:found)
1	964.9:965.4
2	1078.1:1078.4
3	1191.3:1191.5

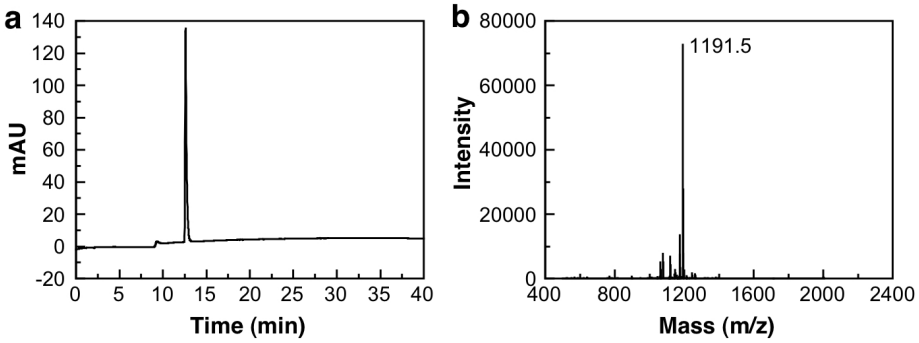

Figure S1. (a) Analytic HPLC profile and (b) MALDI mass spectrum for the compound **3**.

Protein expression and purification for a his_6-tagged red fluorescent protein mCherry and the cleavage of his_6-tag. Dr. Caroline Ajo-Franklin (LBNL) provided us a *E. Coli* strain that overexpress the his_6-tagged mCherry.[2] The expression plasmid has a thrombin-cleavage site after N-terminal his_6-tag. The *E. Coli* strain were grown in LB medium with shaking at 37°C until the OD_{600} reached 0.5. Then, the mCherry was over expressed with the addition of 1 mM of IPTG at 37°C for 4–5 h. After the *E. Coli* were harvested by centrifugation, we followed a standard protocol for protein purification that was found elsewhere.[3] We used a 1 ml HisTrap FF column (GE Health Sciences) to purify the mCherry. The purified mCherry was dialyzed with a buffer of 100 mM Tris-

HCl (pH 7.5) and 0.1 M NaCl. The amount of mCherry was quantified using the extinction coefficient of 72000 $M^{-1}cm^{-1}$ at 586 nm. In order to obtain the mCherry without the his_6-tag, we cleaved the purified his_6-tagged mCherry with thrombin using the Thrombin CleanCleave™ Kit from Sigma-Aldrich.

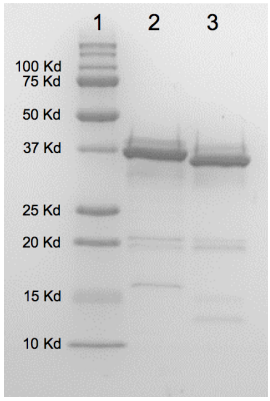

Figure S2. SDS-PAGE for the purified mCherry with his_6-tag (lane 2) and without the tag after thrombin cleavage (lane 3). The size markers with protein standards are shown in lane 1.

Assays for fiber formation, binding of mCherry to the fibers and growth of metal nanoparticles. The modified peptides **1**, **2** and were dissolved in water with 10 mM NaOH as a stock of 4 mM. These compounds were diluted to 0.5 mM in the presence of 20 mM Tris-HCl (pH 7.5), 0.1 M NaCl and 5 mM of metal chloride. The time-dependent aggregation of the compounds was monitored by the absorbance at 450 nm using a 96 well plate reader SPECTRAmax Plus 384 from Molecular Devices (Sunnyvale, CA) with shaking for 20 sec before and after the measurement. The disassembly of the metal-ion induced fibers were also monitored by the same 96 well plate reader after mixing the sample solution with a ratio of 1:1 (v/v) with 100 mM EDTA in the presence of 20 mM Tris-HCl (pH 7.5) and 0.1 M NaCl.

For the binding of mCherry to the fibers, the metal-ion induced fibers were first dialyzed with 20 mM Tris-HCl (pH 7.5) and 0.1 M NaCl for 1 day using Slide-A-Lyzer® mini dialysis unit (7000 MWCO) from Pierce (Rockford, IL) in order to remove excess metal ions. The mCherry was then added to the sample solution with a final concentration

of 3 μM. The binding of mCherry to the fibers was visualized by fluorescence microscopy using the Olympus IX 81 microscope.

For the growth of metal nanoparticles, the reducing reagent sodium borohydride was added to the sample solutions of metal-ion induced fibers with a final concentration of 7 mM. After 30 min of incubation, the samples were prepared for electron microscopy.

Samples for electron microscopy were prepared by mounting a droplet of fibril solution to 400 mesh carbon support film on copper grid from the Electron Microscopy Sciences (Hatfield, PA). The grids were then washed with two times of water droplet, stained with 2% uranyl acetate and dried. For the images of metal nanoparticles, we skipped the staining step. All specimens were examined in transmission mode - scanning electron microscope (TM-SEM) at an accelerating voltage of 30 kV using Zeiss Gemini Ultra-55 Analytical Scanning Electron Microscope. For high-resolution TEM (HRTEM), the images were obtained using JEOL 2100-F 200 kV Field-Emission Analytical Transmission Electron Microscope. The software ImageJ 1.42q (Wayne Rasband) was used in order to obtain the size distribution of the metal nanoparticles.

We measured X-ray diffraction for metal-ion induced fibers in order to see if there is a regular molecular spacing in the fibers. The fibers were first centrifuged, washed with water and then dried. The dried samples were mounted on the sample loop to hold the aggregated fibers. We used the beamline BL 8.3.1 at Advanced Light Source in Lawrence Berkeley National Laboratory.

References

1 R. N. Zuckermann, J. M. Kerr, S. B. H. Kent and W. H. Moos, *J. Am. Chem. Soc.* 1992, **114**, 10646.
2 C. M. Ajo-Franklin, D. A. Drubin, J. A. Eskin, E. P. S. Gee, D. Landgraf, I. Philips and P. A. Silver, *Genes Dev.* 2007, **21**, 2271.
3 E. R. Ballister, A. H. Lai, R. N. Zuckermann, Y. Cheng and J. D. Mougous, *Proc. Natl. Acad. Sci. U. S. A.* 2008, **105***,* 3733.

Scanning electron microscopy images for metal-ion induced fibers from compound 2 and 3.

Figure S3. Scanning electron microscopy images from (a) Cu(II)-, (b) Co(II)-, (c), Zn(II)-, (d) Ni(II)- and (e) Mn(II)-induced fibers with compound **2**. The black scale bar in the left positive image: 200 nm. The white scale bar in the right negative image: 2 μm.

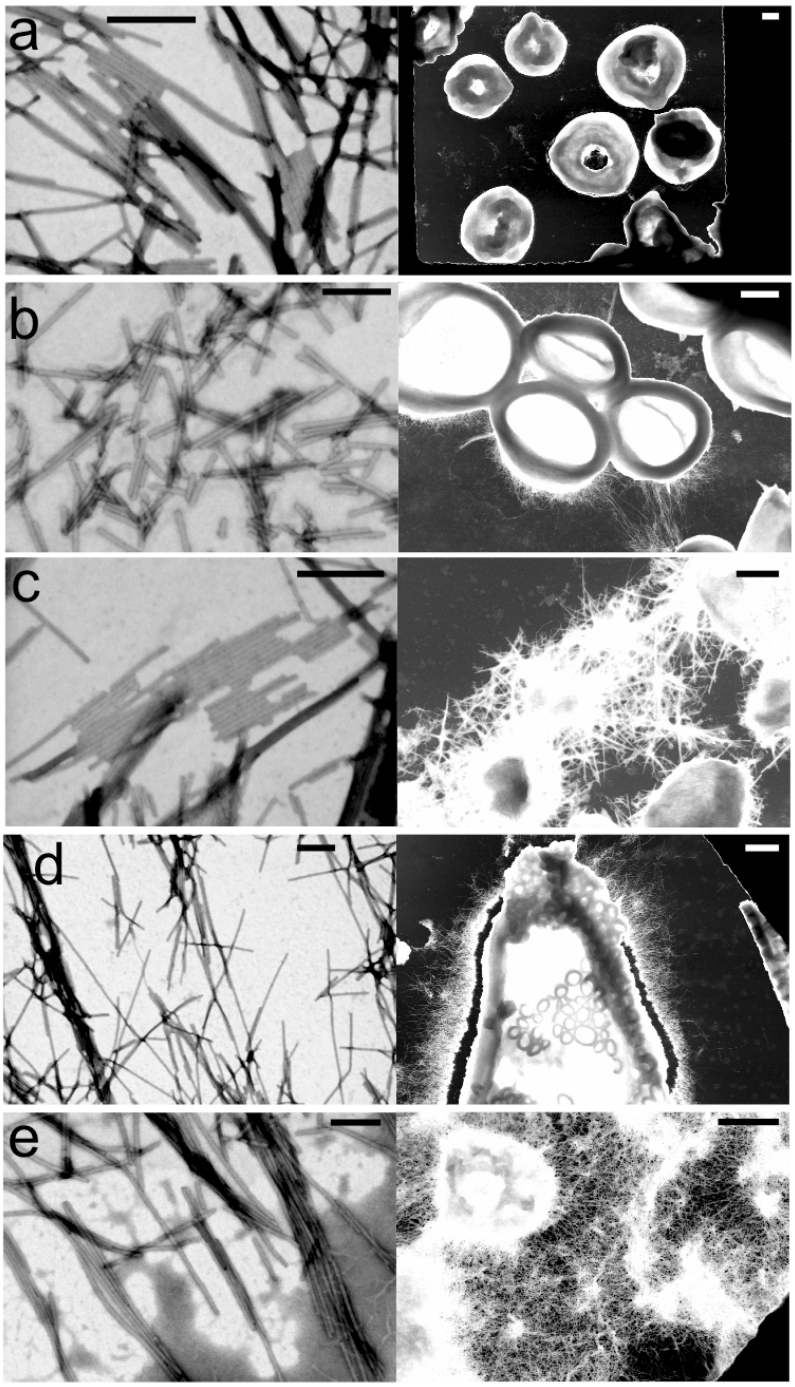

Figure S4. Scanning electron microscopy images from (a) Cu(II)-, (b) Co(II)-, (c), Zn(II)-, (d) Ni(II)- and (e) Mn(II)-induced fibers with compound **3**. The black scale bar in the left positive image: 200 nm. The white scale bar in the right negative image: 2 μm. The metal fibers from compound **2** and **3** stick to each other to form higher order, donut-shaped super-structures of clumped fibers as shown in low magnification images. The size of the donut-shaped clumps varied in a range from 1 to 10 microns. We believe that the heterogeneity in fiber-forming kinetics generates different lengths of fibers, and metal ions bring those fibers together to accommodate this donut-shape.

X-ray power diffraction data for metal-ion induced fibers.

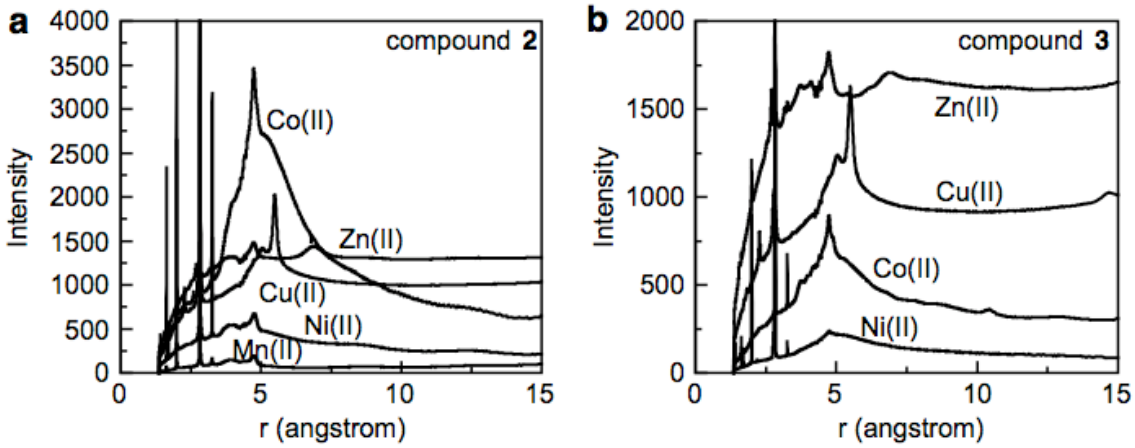

Figure S5. Molecular spacing obtained by powder X-ray diffraction. (a) metal-ion induced fibers from the compound **2** and (b) metal-ion induced fibers from the compound **3**.

Binding of mCherry to the metal-ion induced fibers from compound 2.

QuickTime™ and a
decompressor
are needed to see this picture.

Figure S6. Fluorescence microscopy images showing the binding of mCherry to (a) Co(II)-induced fibers and (b) Ni(II)-induced fibers from compound **2**.

Binding of mCherry (lacking his_6 tag) to the fibers.

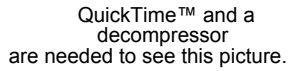

Figure S7. Bright field (left panel) and fluorescence microscopy images (right panel) of (a) Co(II)- and (b) Ni(II)-induced fibers from compound **2** with addition of non-his_6 tagged mCherry, and (c) Co(II)- and (d) Ni(II)-induced fibers from compound **3** with addition of non-his_6-tagged mCherry.

Size distribution of Cu and Ni nanoparticles generated by compound 3.

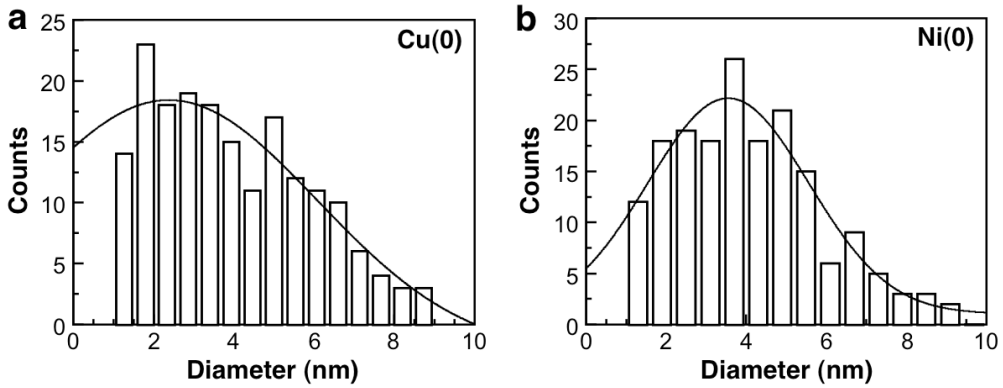

Figure S8. Histogram of (a) Cu and (b) Ni nanoparticles raised by the reduction of each correspondent metal ion with fibers from compound **3**. The data were fit by Gaussian model with mean values of 2.4 ± 0.8 and 3.6 ± 0.2 nm, and standard deviations of 5.2 ± 2.8 and 2.8 ± 0.4 for Cu and Ni nanoparticles, respectively. Averaged diameters are 4.0 nm and 4.1 nm, and standard deviations are 1.9 nm and 1.8 nm for Cu and Ni nanoparticles, respectively.

High-resolution TEM images of metal nanoparticles.

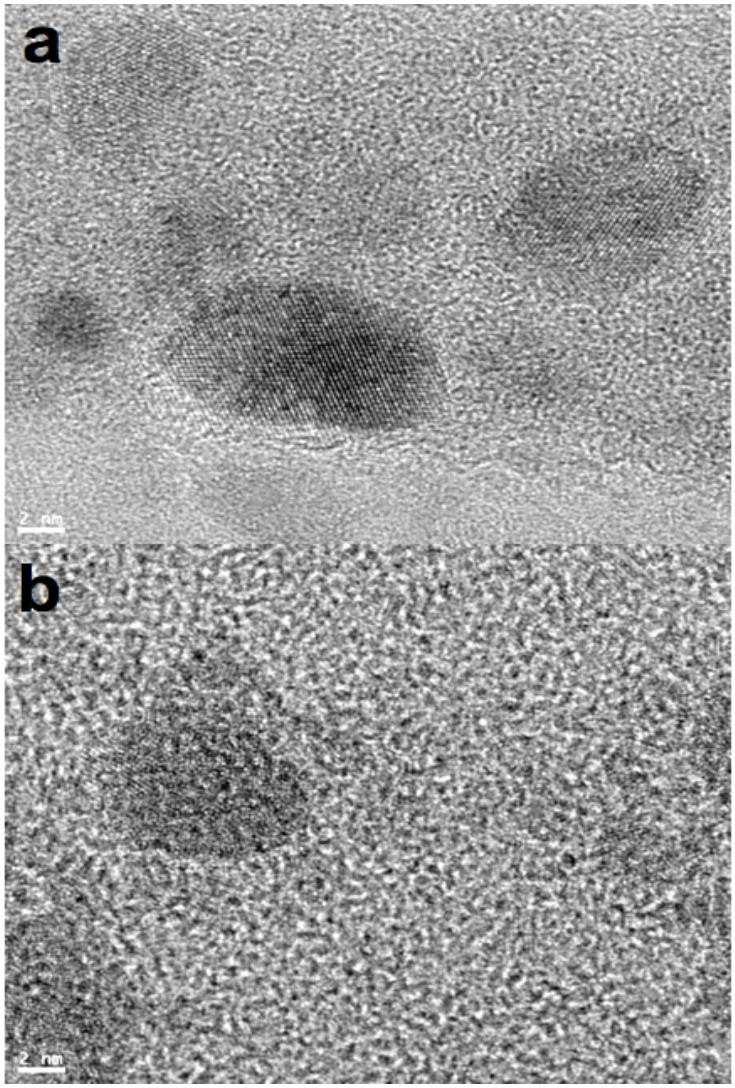

Figure S9. High-resolution TEM images of (a) Cu and (b) Ni nanoparticles grown from the corresponding metal ions with the fibers from compound **3**. The HRTEM image of Cu nanoparticles showed a clear regular array of atoms, but the degree of crystallization of Ni nanoparticles is less clear, but did contain domains of crystal lattice.